

Paleoclimatic variations in foraminifer assemblages from the Alboran Sea (Western Mediterranean) during the last 150 ka in ODP Site 977

M. Pérez-Folgado^{a,*}, F.J. Sierro^a, J.A. Flores^a, J.O. Grimalt^b, R. Zahn^c

^aDepartment of Geology, University of Salamanca, Plaza de la Merced s/n 37008, Salamanca, Spain

^bDepartment of Environmental Chemistry, Institute of Chemical and Environmental Research (CSIC), Jordi Girona, 18, 08034 Barcelona, Spain

^cG.R.C. Marine Geosciences, Department of Stratigraphy and Paleontology, University of Barcelona, 08071 Barcelona, Spain

Received 4 March 2003; received in revised form 18 May 2004; accepted 26 August 2004

Abstract

Detailed analysis of the planktonic foraminifera assemblages of ODP Site 977, situated in the Alboran Sea (36°1,9'N; 1°57,3'W), led us to recognize 42 planktonic foraminiferal events that occurred during marine isotope stages (MIS) 4 and 5. These events were defined by changes in the abundances of *Neogloboquadrina pachyderma* (right and left coiling), *Turborotalita quinqueloba*, *Globorotalia scitula*, *Globorotalia inflata*, *Globigerina bulloides* and *Globigerinoides ruber* (white and pink varieties). Foraminiferal assemblages changed in response to glacial–interglacial and millennial climate variability throughout the last 150 ka. Based on the estimation of sea surface temperatures (SST) using the modern analog technique and the oxygen isotope data measured in *G. bulloides*, we inferred the oxygen isotopic composition of sea water (δw). SST increased in the Alboran Sea during the main Dansgaard–Oeschger Interstadials, such as interstadial 19 to 24. Even though *N. pachyderma* (left coiling) is very scarce before Heinrich Event (HE) 6, three cold pulses can be identified, between 65 and 85 ka ago. Moreover, increases in abundance of *T. quinqueloba* and *G. scitula* are recorded during D–O Stadials 20 and 21.

The maximum temperature, which was attained during the Last Interglacial, was about 2 °C higher than recent temperature and that reached over the Holocene. Planktic foraminifera assemblages and paleotemperatures remained cold 3 ka after the beginning of Termination II (T-II), 130 ka ago, probably in connection with the occurrence of Heinrich event 11 in the North Atlantic.

The abundance of *G. bulloides* during the deposition of organic rich layers (ORLs) of MIS 5, accompanied by lower isotope values in surface waters (δw), could indicate the presence of a fresher surface layer associated with an increase in marine surface productivity.

© 2004 Elsevier B.V. All rights reserved.

Keywords: organic rich layers; Alboran Sea; marine isotope stage 5; planktic foraminifera; paleotemperatures; millennial variability

* Corresponding author. Tel.: +34 923 294497; fax: +34 923 294514.

E-mail address: martap@usal.es (M. Pérez-Folgado).

1. Introduction

The Alboran Sea, situated in the western margin of the Mediterranean basin, connects the Atlantic Ocean with the Mediterranean Sea, providing an exceptional site to record both Atlantic and Mediterranean paleoclimatic and paleoceanographic events. In the Alboran Sea, the inflow Atlantic Water (Modified Atlantic Water; MAW) forms two anticyclonic gyres (Fig. 1) that fill the first 150–200 m (Parrilla, 1984; Heburn and LaViolette, 1990). The Mediterranean Water is flowing westward below the MAW, and is divided into two different water masses: the Levantine Intermediate Water (LIW), which is formed in the eastern Mediterranean Sea, forms the main component of the Mediterranean Outflow Water (MOW) at the Strait of Gibraltar; and the Western Mediterranean Deep Water (WMDW), which is formed in the Gulf of Lyons, extends from around 600 m to the bottom of the basin, and contribute sporadically to the MOW (Kinder and Parrilla, 1987; Parrilla and Kinder, 1987).

Although the Mediterranean is an oligotrophic Sea, due in part to its negative hydrological budget (Bethoux, 1979), two areas of high productivity are present in the Alboran Sea in connection with the interaction between the MAW and LIW: one in the north part of the western anticyclonic gyre (Bárcena and Abrantes, 1998; García-Gorrioz and Carr, 2001),

and the other one in the eastern part of the basin, the Almería–Orán front (Fig. 1; Tintoré et al., 1988).

During the last glacial period, the Mediterranean Sea underwent rapid oscillations in hydrographic conditions owing to abrupt climatic changes recorded in the Northern Hemisphere, known as Heinrich events (HE) and Dansgaard–Oeschger (D–O) Stadials (cold) and Interstadials (warm) (Heinrich, 1988; Dansgaard et al., 1993). HE are linked with maximum oceanic cooling during the rapid atmospheric climatic fluctuations defined in ice cores from Greenland (Dansgaard et al., 1993; Grootes et al., 1993), known as D–O cycles. Cacho et al (1999) proved that these variations in atmospheric temperature over Greenland were linked to changes in sea surface temperature (SST) of the Alboran Sea. During marine isotopic stage (MIS) 3, the winter sea surface temperature dropped to around 7 °C during HE and rose to values close to 13 °C during the most important D–O Interstadials (Cacho et al., 1999). Furthermore, changes in the foraminiferal assemblages of the Alboran Sea, especially during MIS 3, were related to HE and D–O cycles (Pérez-Folgado et al., 2003). In addition, deep-water circulation in the Western Mediterranean was very active during D–O Stadials and HE, but slowed down during D–O Interstadials (Cacho et al., 2000).

Excellent climatic records for the last 110 ka have been recovered in the GRIP as well as in the GISP2

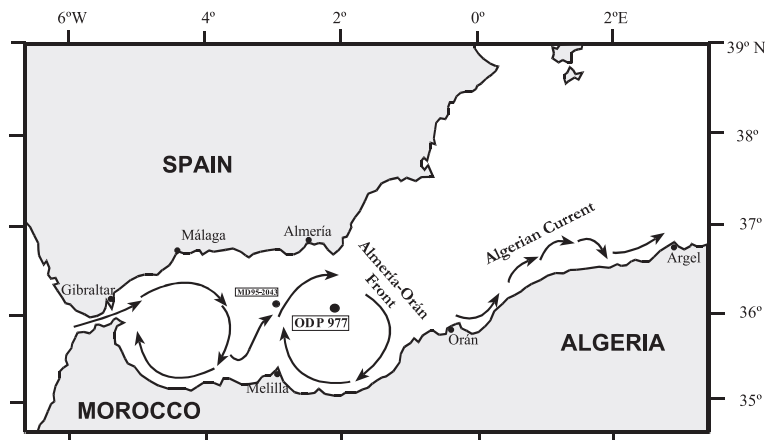


Fig. 1. Map showing the situation of ODP 977 in the Alboran Sea. The major paths of Modified Atlantic Water (MAW) in the Western Mediterranean are also shown.

Greenland ice cores. However, for older ages (MIS 5 and 6), there are no ice core records available for the Northern Hemisphere. Nevertheless, some studies carried out in deep-sea sediments from the North Atlantic revealed that the millennial variability recorded in Greenland during MIS 1 to 4 continued during older isotopic stages (McManus et al., 1994; Chapman and Shackleton, 1998; 1999; Sánchez-Goñi et al., 1999; 2002; Oppo et al., 2001).

MIS 3 millennial changes have been recorded in both Hemispheres (e.g., Dansgaard et al., 1993; Bond et al., 1993; Hüls and Zahn, 2000; Little et al., 1997; Kanfoush et al., 2000; Cacho et al., 1999), so they can be considered very widespread events (see review in Voelker et al., 2002 and in Rohling et al., 2003). However, it is during marine isotopic stages 3 and 4 where this variability is best recorded, and not during the Holocene or MIS 5. This could be due to the smaller size of the ice sheets during interglacial episodes (McManus et al., 1999).

The penultimate deglaciation took place around 130 ka ago (Martinson et al., 1987), but Termination II (T-II) structure, Last Interglacial stability, and the influence of sub-Milankovitch variability are still controversial aspects (GRIP members, 1993; McManus et al., 1994; Alley et al., 1995; Lauritzen, 1995; Seidenkrantz et al., 1995; Oppo et al., 1997; Chapman and Shackleton, 1999; Sánchez-Goñi et al., 2000).

Over the past few million years, the Mediterranean Sea has been very sensitive to orbital climate change as demonstrated by the cyclic deposition of organic-rich, laminated sediments, known as sapropels (Bradley, 1938; Kullenberg, 1952; Ryan et al., 1973; Hsü et al., 1978; Kidd et al., 1978; Rossignol-Strick, 1985; Vergnaud-Grazzini et al., 1986; Ganssen and Troelstra, 1987; Bethoux, 1993; Rohling, 1994; 1999; Emeis et al., 1996; Comas et al., 1996; Meyers and Negri, 2003; Sierro et al., 2003). The most recent sapropels (S5–S1) are very well defined and documented for the eastern Mediterranean (Rohling, 1994), whereas in the western part (from the Gibraltar Strait to Sicily), these events are not recorded, but organic-rich, nonlaminated layers (ORL) were deposited instead, sensu Comas et al. (1996).

The present work has two principal objectives. First, to attempt to define a high-resolution biostratig-

raphy based on planktic foraminiferal events, for MIS 4 and 5, in the Alboran Sea that could be useful for elaborating a stratigraphic framework for the Western Mediterranean. Second, to evaluate the oceanographic and climatic changes that have occurred in this area of water exchange between the Atlantic Ocean and the Mediterranean. We report results on planktic foraminiferal assemblages, stable isotopes ($\delta^{18}\text{O}$ and $\delta^{13}\text{C}$), paleotemperatures and δw records in 288 samples of the core ODP Site 977 recovered in the Alboran Sea (Fig. 1).

2. Materials and methods

Site 977 is located South of the Cabo de Gata, in the Western basin of the Alboran Sea (Fig. 1), halfway between Spain and the Algerian coast ($36^{\circ}1,9'N$; $1^{\circ}57,3'W$) at a water depth of 1984 m. The core (~600 m length) is divided into two units (I and II). In this study, we analyzed the first 27.24 m of Unit I. The dominant lithologies are nannofossil and calcareous silty clay and clay. Unit I is characterized by the presence of discrete organic rich layers (ORLs), which comprise 8.5% of the stratigraphic section of the first 253 m of core ODP 977. We found eight of these ORLs in our samples (L1–L8), with TOC values ranging around 0.8–1% (Types II and III). The background TOC value is 0.55% for the whole core. ORLs are greenish in color and exhibit low magnetic susceptibilities (Comas et al., 1996).

We studied 288 samples—approximately one sample per 10 cm—with an average resolution of about 450 years. Some of the results concerning the first 180 samples (mainly faunal results) are yet published elsewhere (Pérez-Folgado et al., 2003), and we here offer the planktic foraminiferal data for the rest of the samples and some new results (e.g., paleotemperatures) for the total length.

Samples were prepared in the laboratory, using the procedure described below.

The samples for the analysis of planktic foraminiferal assemblages were washed through a 62- μm sieve and dry-sieved again through a 150- μm mesh. The residues ($>150\ \mu\text{m}$) were split the number of times necessary to obtain an aliquot fraction of some 400 specimens (average of 431), which were counted and identified. To calculate the abundance of *Neoglobob-*

quadrina pachyderma left coiling (l.c.), an aliquot of around 1000 specimens (average of 1037) was analyzed. Oxygen and carbon isotope measurements were performed on the planktic foraminifer *Globigerina bulloides*, on the 250–355- μm fraction. Samples were measured on a Finnigan MAT 251 device at the University of Kiel.

Seasonal paleotemperatures were obtained using the modern analog method (MAT; Hutson, 1980; Prell, 1985). This method uses a statistical distance (in our case, the ‘squared chord distance’; Overpeck et al., 1985) called the ‘dissimilarity index’, which gives the relationship between fossil and current assemblages. This index varies between 0.0 and 0.4. Normally, a dissimilarity lower than 0.2 is taken as the limit for a good reconstruction. The final paleo-SST is the weighted mean of the 10 best analogs. The database used here was that of Kallel et al. (1997a) for the Mediterranean Sea, which comprises 253 coretop samples (128 from the Mediterranean Sea and 123 from the North Atlantic Ocean). The average ‘dissimilarity’ obtained was 0.13, and the mean error for all the reconstructions was ± 2 °C.

3. Age model

Pérez-Folgado et al. (2003) first established an age model from 0 to 70 ka for ODP 977, mainly based on its correlation with the nearby well-dated core MD95-2043 (Cacho et al., 1999). Moreover, there are two ^{14}C -AMS dating for the Late Holocene (Table 1). However, since core MD95-2043 only extends to 54 ka ago, here we establish a new age model valid for the entire interval studied (0–150 ka), based only in part on previous one (Table 1).

To construct this new age model, we assumed that the $\delta^{18}\text{O}_{G. bulloides}$ record mostly reflects sea surface temperature variability in the Alboran Sea, which is synchronous with millennial variability in air temperature as recorded in Greenland. For the first 18 m of the core (~80 ka), we correlated the $\delta^{18}\text{O}_{G. bulloides}$ data with $\delta^{18}\text{O}$ from ice cores in Greenland (Fig. 2A,B). However, Greenland ice core records are controversial for ages older than ~100 ka (e.g., Alley et al., 1995) and therefore for the older part of ODP 977 core we compared our $\delta^{18}\text{O}$ curve with the SPECMAP stack curve of Martinson et al. (1987), and

Table 1
Age model pointers for ODP core 977

Event	Depth ODP 977(m)	Age Specmap (years)	Reference
^{14}C -AMS	0.202	1159	Pérez-Folgado et al. (2003)
^{14}C -AMS	0.605	4220	Pérez-Folgado et al. (2003)
Base B/A	2.900	14,836	Pérez-Folgado et al. (2003)
HE 1	3.144	16,320	Pérez-Folgado et al. (2003)
Base IS 8-A1	7.615	37,010	(*)
Base IS 12-A2	9.460	42,880	(*)
Base IS 14-A3	11.058	50,350	(*)
Base IS 17-A4	11.885	57,050	(*)
MIS 4.0	12.135	58,960	Martinson et al. (1987)
Base IS 19-A5	14.083	67,700	(*)
Base IS 20-A6	15.736	70,800	(*)
MIS 5.0	16.150	73,910	Martinson et al. (1987)
Base IS 21-A7	18.123	79,260	(*)
MIS 5.2/5.3	19.396	93,145	Martinson et al. (1987)
MIS 5.31	19.514	96,210	Martinson et al. (1987)
MIS 5.33	20.848	103,290	Martinson et al. (1987)
MIS 5.4/5.5	22.070	117,300	Martinson et al. (1987)
MIS 5.53	23.593	125,000	Martinson et al. (1987)
MIS 6.0	24.339	129,840	Martinson et al. (1987)
MIS 6.2	25.277	135,100	Martinson et al. (1987)
MIS 6.2/6.3	26.305	139,020	Martinson et al. (1987)
MIS 6.3	26.645	142,280	Martinson et al. (1987)

(*) Sowers et al. (1993); Schwander et al. (1997); Blunier and Brook (2001).

See Table 2 for details. B/A: Bölling-Allerod. HE: Heinrich Event. IS: Greenland Interstadial. A1–A7: Antarctic warmings. MIS: marine isotopic stage.

recognized some age pointers (Table 1; Fig. 2D). In order to maintain the coherence between the lower and the upper part of our age model, we converted the ice ages into SPECMAP ages (Tables 1 and 2), using the procedure described below.

Sowers et al. (1993) estimated SPECMAP ages for the Vostok (Antarctica) ice core. They compared the $\delta^{18}\text{O}$ age of O_2 included in ice air bubbles with the $\delta^{18}\text{O}$ record obtained in the benthic foraminifer *Uvigerina senticososa* in a deep-ocean core (Table 2). They took into account 2 ka for the mixing time of the oxygen in the atmosphere. Blunier and Brook (2001) correlated methane records (CH_4) in ice air bubbles between Antarctica (Byrd ice core) and Greenland (GRIP and GISP2 ice cores). They assumed that these methane records must be isochronous, owing to the rapid diffusion of this gas in the atmosphere (~1 year). The correlation revealed that the warmings in Antarctic ice cores during MIS

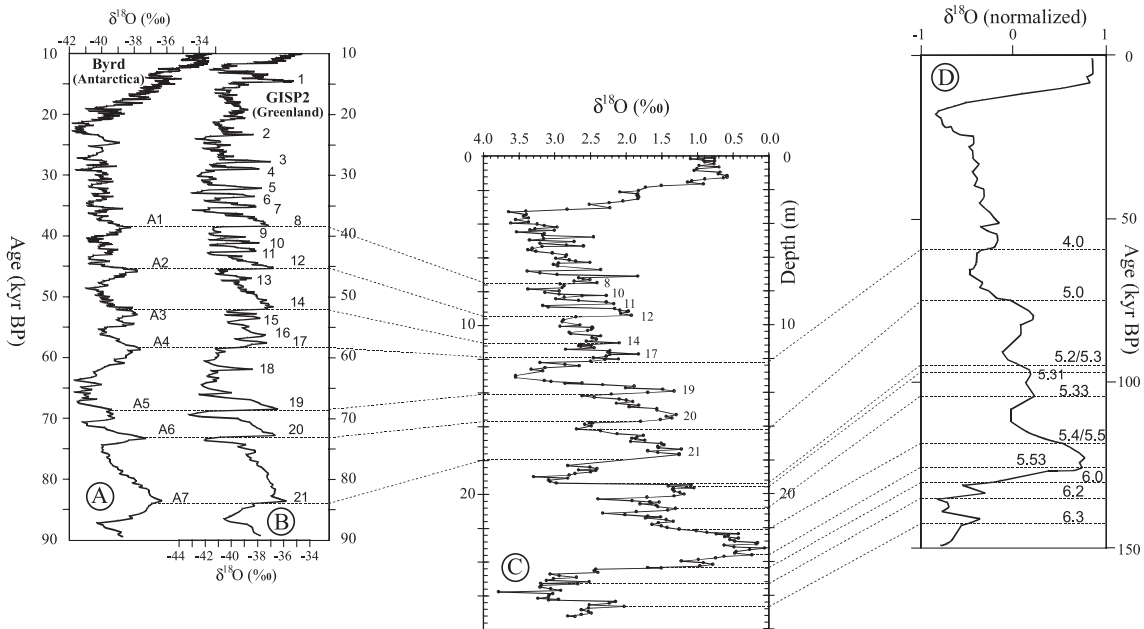


Fig. 2. Proposed age model for first 28 m of ODP Site 977. Curves (A) and (B) are from Blunier and Brook's (2001) comparison of ice cores. (C) $\delta^{18}\text{O}$ data from ODP 977 and (D) $\delta^{18}\text{O}$ SPECMAP curve of Martinson et al. (1987). See text for details concerning the age model.

3 (A1–A7; Fig. 2, Table 2) coincided with terminations of Dansgaard–Oeschger Stadials in Greenland, and not with the Interstadials (Blunier and Brook, 2001). In the $\delta^{18}\text{O}_{G. bulloides}$ data of our core ODP 977, as in the alkenones SST paleo-record (López et al., in preparation) and in the planktic foraminifera fauna (Pérez-Folgado et al., 2003), D–O cycles were identified. We assigned SPECMAP ages to these cycles through their synchronization with

events A1 to A7 recorded in Vostok, using the SPECMAP ages of Sowers et al. (1993) (Tables 1 and 2). However, there is an age offset (Δage) between the gas age and the ice age, because the air is trapped in bubbles normally lying 50–100 m below the ice surface; hence, the trapped air is younger than the surrounding ice (Schwander et al., 1997). Accordingly, the final step to transform A1–A7 ice ages into SPECMAP ages was to add this Δage (Schwander et al., 1997) to the SPECMAP gas age (Table 2).

Table 2

Steps to obtain SPECMAP ages of the Interstadials D–O 8 to 21 as recorded in ODP977

A	B	C	D	E	F
A1	IS 8	7.615	36.5	0.51	37.01
A2	IS 12	9.460	42.4	0.48	42.88
A3	IS 14	11.058	49.9	0.45	50.35
A4	IS 17	11.885	56.5	0.55	57.05
A5	IS 19	14.083	67.3	0.40	67.70
A6	IS 20	15.736	70.4	0.40	70.80
A7	IS 21	18.123	79.0	0.26	79.26

A: A1–A7 Antarctic warmings of Blunier and Brook (2001) B: base of the equivalent Greenland Interstadial (IS). C: ODP 977 depth (m) for these events. D: Vostok SPECMAP gas age (Sowers et al., 1993). E: Δage (Schwander et al., 1997). F: SPECMAP ages for A1 to A7 (D+E). All ages are in kiloyears.

4. Results

4.1. Faunal results

In ODP 977, all the planktic foraminifera species were identified and counted, included the coiling types of *N. pachyderma* (left and right coiling), and both varieties of *Globigerinoides ruber* (white and pink). Thus, we finally obtained eight significant types (Fig. 3). Pérez-Folgado et al. (2003) previously defined faunal bioevents in the upper part of this core, based in part on those of Pujol and Vergnaud-Grazzini

(1989). All these bioevents, together with those reported here for MIS 4, 5 and part of MIS 6, are shown in Fig. 3. In Table 3, we show the age intervals for each event, according to our age model. Benthic foraminifera are almost absent during part of sub-stages 5e, 5d, 5a and MIS 4. During the Holocene, benthics are also very scarce. However, they reach higher percentages (a maximum of 21% of the total foraminifera) during MIS 3 and some parts of MIS 4, 5 and 6 (Fig. 4).

4.1.1. *Neogloboquadrina pachyderma* (right coiling)

During the last 150 ka, this species has been the principal component of the planktic foraminiferal assemblage in the Alboran Sea, with an average abundance of 44.8%. However, in the current Alboran Sea, and as from ~5 ka ago, this species is only a minor component (3%). Today, its abundance is the lowest from the Last Interglacial, when it reached only 2% of the total assemblage (Fig. 3a).

Different bioevents have been defined by Pujol and Vergnaud-Grazzini (1989) (Pm, P1–P4) and by Pérez-Folgado et al. (2003) (Pm2, Pm3, P5, P6 and SFDZ–Small Foraminifera Dominance Zone). From P6 downward, we define two new minima (Pm4 and Pm5) and four new maxima (P7, P9, P10 and P11) as seen in Fig. 3a and Table 3. Between Pm4 and Pm5 (i.e., between 120 and 75 ka ago), *N. pachyderma* (r.c.) increased its abundance, from an interval with an average of ~29% up to an interval with an average of ~60% (Fig. 3a). P8 marks, at around 100 ka, this change in the tendency.

4.1.2. *Globigerina bulloides*

This species is relatively abundant in the present assemblages (~40%), but during the last six isotopic stages the average abundance was around 25%, some maxima reaching 65%. Apart from the events described previously (Pujol and Vergnaud-Grazzini, 1989; Pérez-Folgado et al., 2003), we define nine significant changes in the abundance of

this species (B7–B15), during MIS 4 and 5 (Fig. 3b, Table 3).

4.1.3. *Turborotalita quinqueloba*

The average abundance of this species is only 8.6% along the samples studied, although most of the variability is centered in MIS 3, with maxima higher than 50% (event Q6; Pérez-Folgado et al., 2003), and an average of 24% for this isotopic stage. First, we lengthen the event Q8 of Pérez-Folgado et al. (2003) because the new samples considered in our work show that Q8 continued down. We define Q9, Q10, Q11 and only the top of Q12, since a downcore study could change the definition of Q12 limits (Fig. 3c).

4.1.4. *Globorotalia scitula*

The highest abundances of this species do not surpass 20% of the total assemblage (Fig. 3d). However, variations are particularly interesting during MIS 3 (e.g., SFDZ; Pérez-Folgado et al., 2003). From MIS 4, we define two new faunal events (Sc7 and Sc8, Table 3) and only the beginning of Sc9, for the same reason that Q12.

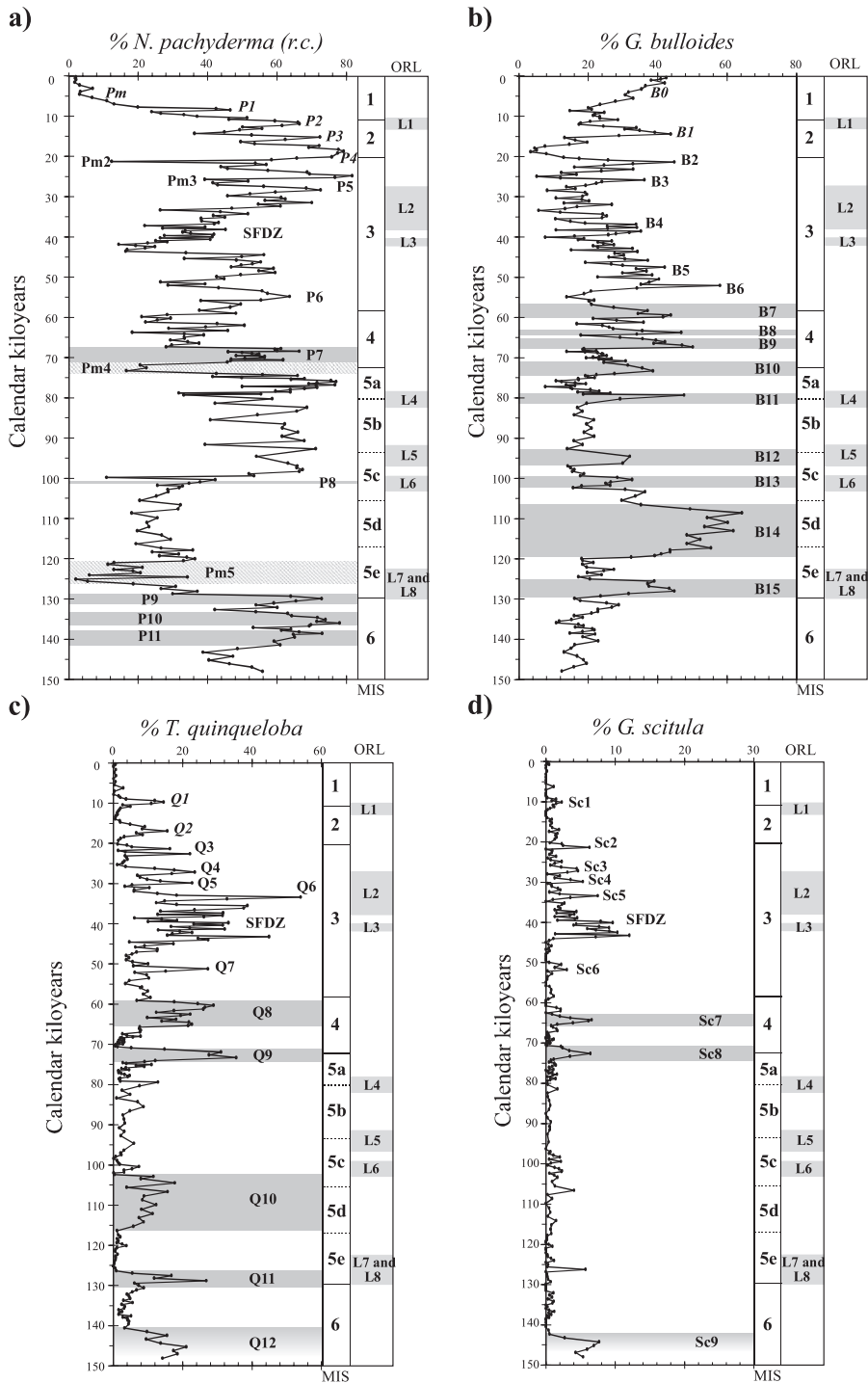
4.1.5. *Globorotalia inflata*

G. inflata is currently one of the principal components of the planktic foraminiferal assemblage in the Alboran Sea, but in the Late Pleistocene the average was only 5.7%. Thus, in general, this species is not very abundant, except in some periods where its abundance increases, defining 11 bioevents for the last two climatic cycles. Of these, here we report those from I6 to I11, during MIS 5, and part of MIS 6 (Fig. 3e, Table 3). The first five prominent events were defined by Pujol and Vergnaud-Grazzini (1989) and by Pérez-Folgado et al. (2003).

4.1.6. *Neogloboquadrina pachyderma* (left coiling)

Pérez-Folgado et al. (2003) identified six characteristic variations in the abundance of this polar

Fig. 3. Quantitative variations in planktonic foraminiferal assemblages in core ODP 977. The first column at the right of the figure marks the presence and the number of the different Organic-Rich Layers identified in the core (Murat, 1999). The second column shows the different marine isotopic stages and substages of the last 150 ka. The biological zones identified for each species in the core for MIS 4 and 5 are delimited by solid gray bands (maxima in abundance) or striped gray bands (minima in abundance). Events and zones defined by Pérez-Folgado et al. (2003) and Pujol and Vergnaud-Grazzini (1989) (in italics) are also shown. SFDZ: small foraminifera dominance zone. (a) *N. pachyderma* (right coiling); (b) *G. bulloides*; (c) *T. quinqueloba*; (d) *G. scitula*; (e) *G. inflata*; (f) *N. pachyderma* (left coiling). Between 62 and 140 ka, the horizontal scale is exaggerated in order to better show the small increases. (g) *G. ruber* white; (h) *G. ruber* pink.



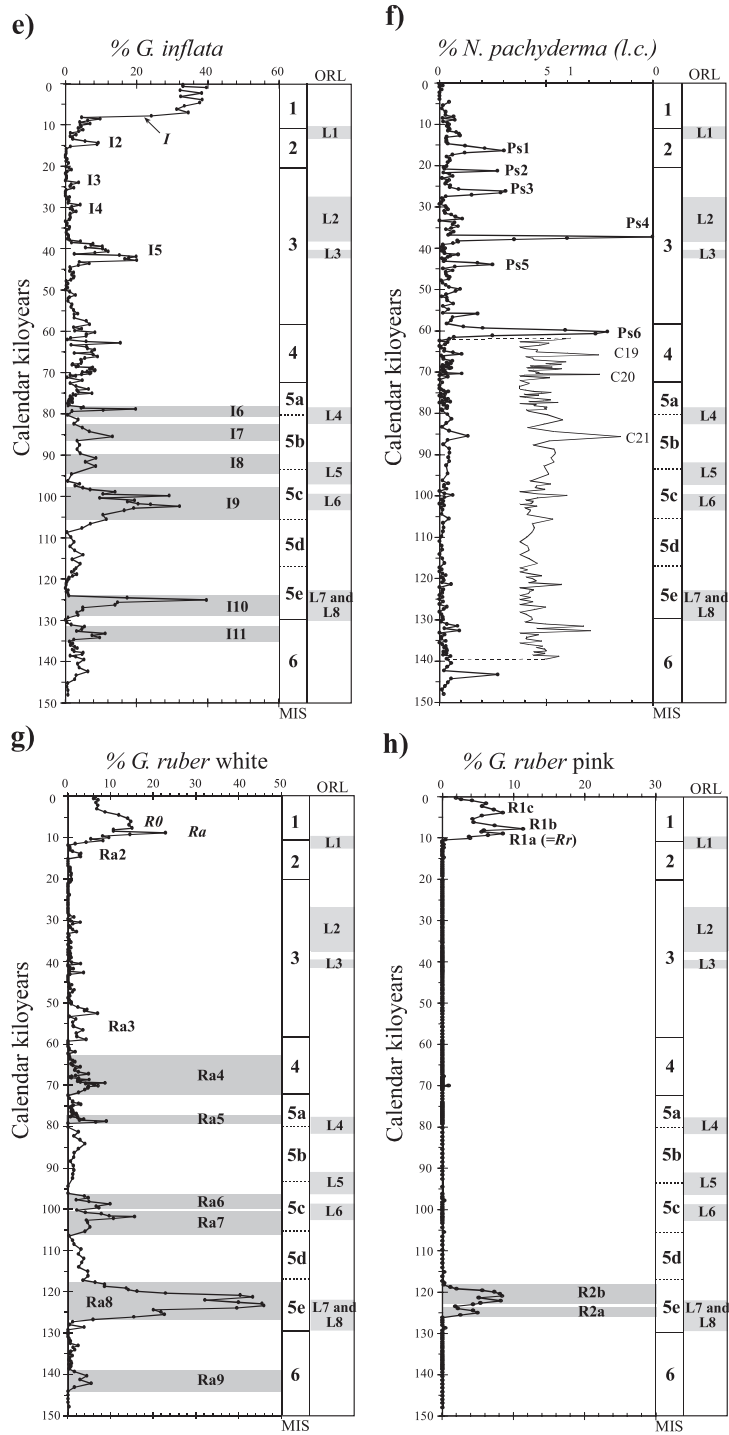


Fig. 3 (continued).

Table 3
Planktic foraminifera zones identified in core ODP 977

<i>G. bulloides</i> zones (figure 3b)	<i>N. pachyderma r.c.</i> zones (figure 3a)	<i>G. inflata</i> zones (figure 3e)	<i>G. ruber white</i> zones (figure 3g)	<i>T. quinqueloba</i> zones (figure 3c)	<i>G. scitula</i> zones (figure 3d)	<i>G. ruber pink</i> zones (figure 3h)
B7 Top 56.7 Max. 59.3 Bottom 60.2	P7 Top 67.3 Max. 68.4 Bottom 71.1	I6 Top 77.9 Max. 78.6 Bottom 79.3	Ra4 Top 63.7 Max. 69.5 Bottom 72.5	Q8 Top 59.1 Max. 60.2 Bottom 65.6	Sc7 Top 62.7 Max. 64.1 Bottom 65.6	R2b Top 118.3 Max. 120.9 Bottom 123.0
B8 Top 62.7 Max. 63.7 Bottom 64.3	Pm4 Top 71.1 Min. 73.2 Bottom 73.9	I7 Top 82.3 Max. 85.4 Bottom 86.4	Ra5 Top 77.7 Max. 78.8 Bottom 79.3	Q9 Top 70.7 Max. 73.2 Bottom 74.4	Sc8 Top 70.5 Max. 72.5 Bottom 74.4	R2a Top 124.0 Max. 125.0 Bottom 126.2
B9 Top 64.9 Max. 67.3 Bottom 67.7	P8 100.1	I8 Top 89.5 Max. 90.6 Bottom 94.5	Ra6 Top 96.2 Max. 98.8 Bottom 99.4	Q10 Top 102.3 Max. 104.3 Bottom 116.2	Sc9 Top 142.3 Max. 144.2	
B10 Top 71.1 Max. 73.2 Bottom 74.2	Pm5 Top 120.4 Min. 125.0 Bottom 126.2	I9 Top 97.8 Max. 102.3 Bottom 105.4	Ra7 Top 101.2 Max. 101.8 Bottom 106.5	Q11 Top 126.2 Max. 128.7 Bottom 131.0		
B11 Top 79.0 Max. 79.3 Bottom 81.3	P9 Top 128.7 Min. 129.8 Bottom 131.4	I10 Top 124.0 Max. 125.0 Bottom 129.3	Ra8 Top 117.3 Max. 123.5 Bottom 127.4	Q12 Top 140.5 Max. 145.1		
B12 Top 92.6 Max. 94.5 Bottom 97.3	P10 Top 133.1 Max. 136.0 Bottom 136.7	I11 Top 131.0 Max. 133.1 Bottom 134.6	Ra9 Top 138.8 Max. 142.3 Bottom 144.2			
B13 Top 99.4 Max. 100.3 Bottom 102.3	P11 Top 137.7 Max. 138.5 Bottom 141.1					
B14 Top 106.5 Max. 108.6 Bottom 119.6						
B15 Top 124.5 Max. 128.0 Bottom 129.8						

All ages are in kiloyears.

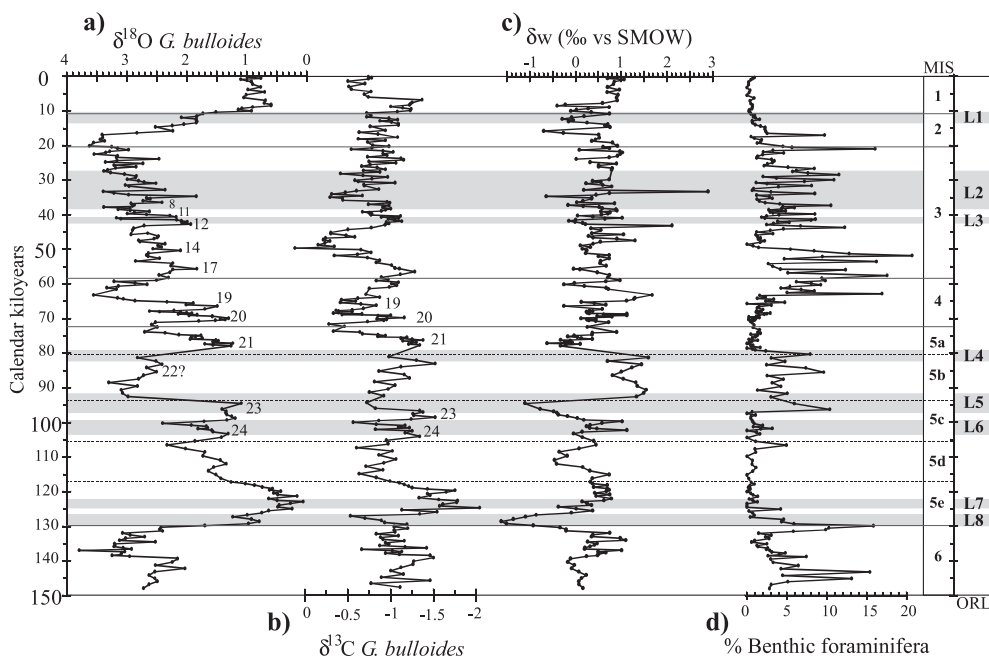


Fig. 4. (a) Oxygen isotope data obtained from *G. bulloides* shells. (b) Carbon isotope data obtained from *G. bulloides* shells. (c) $\delta^{18}\text{O}$ data of the sea water (δ_w). (d) Benthic foraminiferal abundance in ODP 977 (numbers refer to Dansgaard-Oeschger Interstadials).

species (Ps1–Ps6, Fig. 3f), and these can be correlated with the Heinrich Events of North Atlantic Ocean (Heinrich, 1988). From 70 to 150 ka, *N. pachyderma* (l.c.) variations are generally between 0% and 2%. However, at 143.2 ka, we emphasize a small increase of ~3% (Fig. 3f).

4.1.7. *Globigerinoides ruber white*

This warmer-water species only appeared in the Alboran Sea when the surface conditions allowed its growth during the warm stages and substages of the last 150 ka (Fig. 3g). Below Ra3, the last event defined by Pérez-Folgado et al. (2003), we found another six zones (Ra4–Ra9, Table 3). The greatest increase in abundance is seen during the Last Interglacial (event Ra8; Fig. 3g).

4.1.8. *Globigerinoides ruber pink*

This colored variety usually lives in warmer surface waters than the white one, and it only occurred during the warmest periods of the last 150 ka: the Holocene and the Eemian in the Last Interglacial (Fig. 3h). The events recorded during the Holocene have been defined by Pujol and Vergnaud-

Grazzini (1989) and by Pérez-Folgado et al. (2003). Here we define events R2a and R2b, during substage 5e (Fig. 3h, Table 3).

4.2. Isotope results

For the last 150 ka, $\delta^{18}\text{O}$ data on *G. bulloides* vary between values near zero, during the Last Interglacial (substage 5e), to higher than 3.5‰ during cold isotopic stages 2 and 4 (Fig. 4). The record shows all the global climatic changes that occurred during the last two glacial–interglacial episodes. Moreover, the data reflect millennial climatic variability first recorded in the Greenland ice cores (Dansgaard et al., 1993), as may be inferred from the great similarity between the $\delta^{18}\text{O}$ and the SST records. This variability was used to establish the age model (Fig. 2). Termination II is recorded by a 2‰ decrease in $\delta^{18}\text{O}$. After this abrupt change, $\delta^{18}\text{O}$ values increase again (less than 0.5‰) for a short time (1.3 ka), after which they decrease toward the lowest values (near zero) typical of substage 5e. These Eemian values (0–0.6‰) are lower than those recorded in Termination I and the Holocene (between 0.6‰ and 1‰; Fig. 4).

Carbon isotope data ($\delta^{13}\text{C}$; Fig. 4) do not reflect such marked changes as the oxygen data. For the last 150 ka, $\delta^{13}\text{C}$ varies between -2‰ (at 125 ka) and 0.1‰ (at 50 ka). This record is also influenced by millennial variability, especially during MIS 3 (Fig. 4). Generally, $\delta^{13}\text{C}$ decreases when $\delta^{18}\text{O}$ decreases (Fig. 4). However, this is not the case at Termination II, where a sharp decrease in $\delta^{13}\text{C}$ data is recorded at about 127 ka: around 3 ka after the $\delta^{18}\text{O}$ change (at ~ 130 ka).

4.3. Record of SST in ODP 977

Sea surface temperatures (SST) obtained using the modern analog technique (MAT) in the ODP 977 samples are shown in Fig. 5. The average dissimilarity index is 0.13, which is well below the 0.2 limit recommended for a good estimation (Overpeck et al., 1985; Kallel et al., 1997a). Values higher than 0.2 are only found in certain intervals of the past 150 ka (Fig. 5): (i) in the Holocene, around the faunal change between *N. pachyderma* (r.c.) and *G. inflata* (event I; Fig. 3; Pujol and Vergnaud-Grazzini, 1989; Pérez-Folgado et al., 2003), which occurred in the Alboran Sea around 7.7 ka ago; (ii) during MIS 3, mainly in samples with high numbers of *T. quinqueloba* (Q6 event and SFDZ; Fig. 3; Pérez-Folgado et al., 2003), which have no analogs in the modern database. These maxima in *T. quinqueloba* occurred during the major Dansgaard–Oeschger Stadials (Pérez-Folgado et al., 2003); (iii) during MIS 5, in the second half of substage 5e (Last Interglacial). Since the main component of planktic foraminiferal assemblages in these samples is *G. ruber* white, it should be possible to find analogs in the current Eastern Mediterranean assemblage or in the subtropical Atlantic Ocean. However, some of the samples of substage 5e are also rich in other species such as *N. pachyderma* (r.c.) and *G. inflata*, explaining their high dissimilarity. The modern analogs for these samples appear in the central Atlantic, in the Gulf of Biscay, and in the Gulf of Lyons.

The average error of our paleotemperature reconstructions is 2.1 °C , and the standard deviation is $\pm 0.8\text{ °C}$. By seasons, average winter (February SST) error is 1.8 °C ; for spring (April–May SST), it is 1.9

°C ; 2.6 °C for summer (August SST), and 2.2 °C for autumn (October–November SST). The mean annual temperature, which is very similar to the autumn temperature (see Pérez-Folgado et al., 2003), was calculated from the mean of seasonal temperatures, and drawn as a dotted line in Fig. 5.

The coldest temperatures occurred during MIS 4, around 60 ka ago, where values below 7 °C were reached during winter, while the warmest SST were observed in the Last Interglacial during the Eemian. Throughout the year, the paleotemperatures in substage 5e were warmer (by $1\text{--}2\text{ °C}$) than those of the Holocene.

A remarkable offset of around 3 ka is seen between Termination II as inferred from the oxygen isotope record and the warming of Mediterranean surface waters as inferred from the MAT record (Figs. 4 and 5).

4.4. Estimates of sea surface water $\delta^{18}\text{O}$ (δw)

Paleotemperature data were used, together with the oxygen isotope data obtained in *G. bulloides*, to estimate past variations in δw (Fig. 4). We solved the paleotemperature equation of Shackleton (1974) and followed the method of Duplessy et al. (1991) to obtain δw . Spring SST (April–May average) were used because they are the most similar to the current optimum temperature of *G. bulloides* in the Mediterranean Sea (Kallel et al., 1997a). The accuracy of δw estimates depends primarily on that of SST estimates. An error of 1 °C in SST estimates would result in a 0.23‰ error in the calculated δw . An additional error is associated with the mass spectrometric measurements of foraminiferal $\delta^{18}\text{O}$ (Kallel et al., 1997a). The mean spring error is $1.9 \pm 0.8\text{ °C}$; this implies a total error of $0.44 \pm 0.18\text{‰}$ in our δw estimates. Sea water $\delta^{18}\text{O}$ data can be used to obtain paleosalinities, but the high error associated with this method led us to use the δw record as an approach to salinity variations (Rohling, 2000). Fig. 4 shows that δw in the Western Mediterranean Sea changed between -1.5‰ and 3‰ , for the period from 0 to 150 ka. The lowest values are recorded during substages 5c and 5e, associated with ORLs L5 and L8 (Fig. 4), while the highest values occur during MIS 3, cold substage 5b and MIS 6.

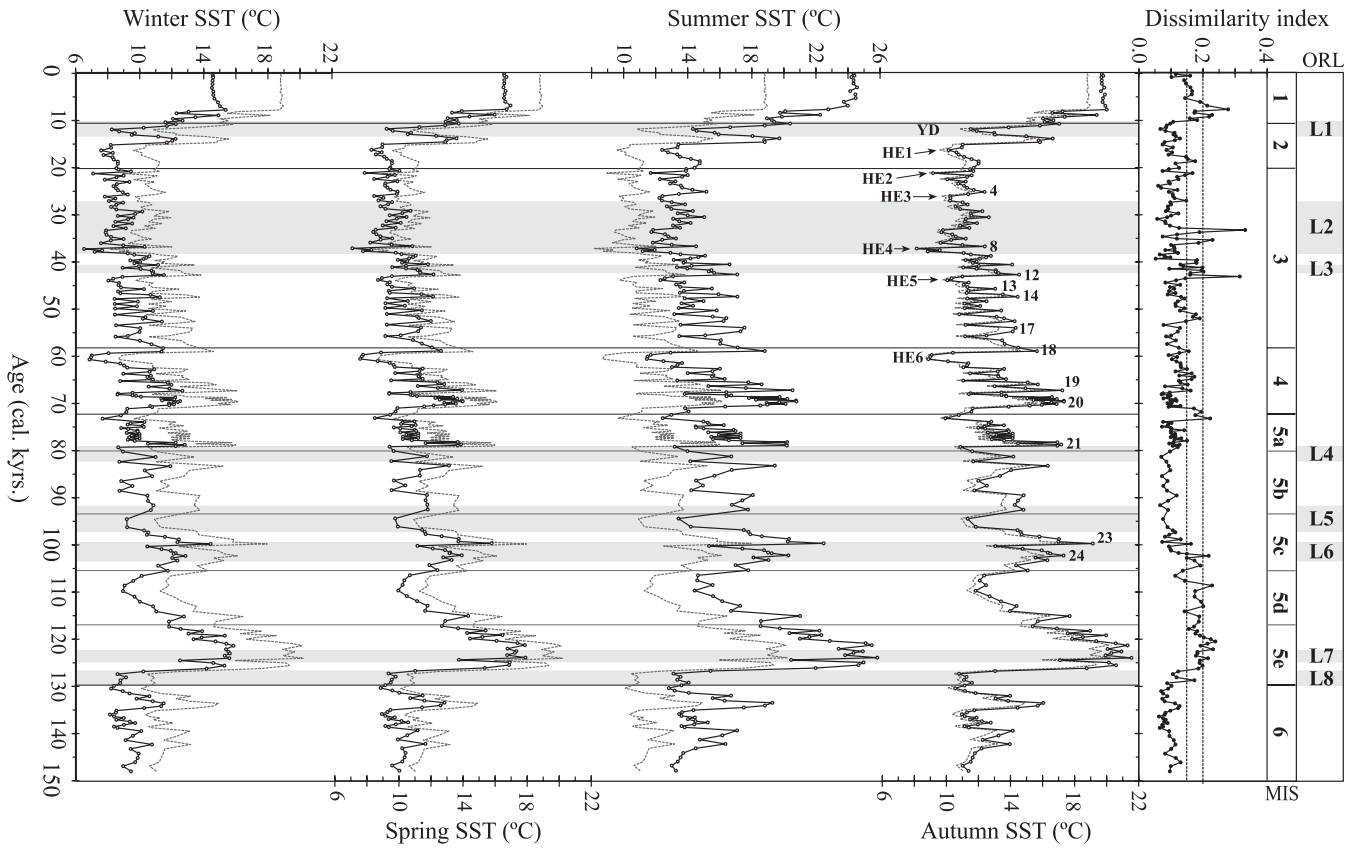


Fig. 5. Paleotemperatures of the last 150 ka in the ODP 977 core, reconstructed using the modern analog technique. The dotted reference lines represent annual mean temperatures. The dissimilarity index of MAT reconstructions is also shown. Winter corresponds to the February temperature; spring is the April–May mean; autumn is the October–November mean, and summer is the August temperature.

5. Discussion

5.1. Response of planktic foraminiferal assemblages to climatic variability in the Alboran Sea during MIS 4 and MIS 5

Planktic foraminiferal assemblages in the Alboran Sea were mainly dominated by *N. pachyderma* (r.c.), *G. bulloides*, *G. ruber* (white and pink varieties), *G. inflata*, and, in warmer periods, some tropical and subtropical species (arranged in the SPRUDTS group; *Globigerinella siphonifera*, *Hastigerina pelagica*, *Globigerina rubescens*, *Orbulina universa*, *Globigerina digitata*, *Globigerinoides tenellus* and *Globigerinoides sacculifer*; Jorissen et al., 1993). This SPRUDTS group can reach around 20% of the association (not represented). Broadly speaking, species abundances vary according to the warm and cold stages and substages of the last 150 ka. Hence, bioevents Ra5 to Ra8 occurred during warm substages 5a, 5c and 5e. *G. ruber* pink maxima (R2a and R2b) only occurred in the warmest epochs, i.e., during the Last Interglacial (Fig. 3), which was also characterized by a prominent minimum in the abundance of *N. pachyderma* r.c. (Pm5). By contrast, Q10 (maximum in *T. quinqueloba*) occurred during cold substage 5d (Fig. 3) associated with an increase in *G. bulloides* (B14). Moreover, both benthic and planktic forams were more abundant, and assemblages were more diverse, during warm periods (substages 5a, 5c and 5e) than during cold ones (substages 5b and 5d).

Abrupt changes in air temperature have been reported to occur in Greenland between 60 and 110 ka (Dansgaard et al., 1993). Dansgaard–Oeschger events 18 to 24 have been recognized during MIS 4 and the younger part of MIS 5, but unfortunately the quality of the ice core records is poor for older ages, preventing the recovery of climatic records for the older part of MIS 5. However, in the North Atlantic, good records of millennial climatic variability extend to MIS 5 and 6 (e.g., Heinrich, 1988; Chapman and Shackleton, 1998; 1999; Cayre et al., 1999; Oppo et al., 2001) and even go back to MIS 12 (McManus et al., 1999).

During MIS 5, below HE 6, several widespread North Atlantic episodes of ice-rafting have been recognized. Heinrich events 8 to 11 were reported

by Heinrich (1988) and later identified by Lehman et al. (2002), Chapman and Shackleton (1998, 1999), Eynaud et al. (2000), Oppo et al. (1997) and Lotoskava and Ganssen (1999). Cayre et al. (1999) defined five coolings (C7 to C11) older than HE 6 in a paleoceanographic reconstruction off the Iberian margin and Chapman and Shackleton (1999) identified seven episodes of ice rafting (C19–C25) between 70 and 126 ka.

Below Heinrich event 6, minor but significant increases of *N. pachyderma* (l.c.) were observed at 65, 70 and 85 ka, which could be related to ice-rafting episodes C19 to C21, defined by Chapman and Shackleton (1999). Other small increases of about 1% between 130 and 132 ka, linked to cold surface waters, can be correlated with HE 11 (Heinrich, 1988), while the small event at 143 ka, although the most pronounced of the period 65–150 ka, does not seem to be related to cool surface temperatures (Fig. 3f, 5).

As already reported for MIS 2 and 3 (Cacho et al., 1999; Pérez-Folgado et al., 2003), the short periods with cool SST temperatures and high $\delta^{18}\text{O}$ in the ODP 977 are linked with cooling events in the Northern Hemisphere, either with Heinrich events or with D–O Stadials. According to the age model, the Mediterranean events of cool surface waters shown in Fig. 5 between ~60 and 105 ka would be correlated with D–O Stadials 19 to 24. Within the relatively cold MIS 4, two intervals of warm temperatures are recorded (Fig. 5). First, SST increased by several degrees (up to 8 °C during summer and only 3 °C during winter) at the beginning of the stage, and a second, lower-amplitude, warm event can be recognized in the middle of MIS 4. These two events are related to Interstadials D–O 20 and 19, as can also be seen in the stable isotope record (Figs. 4 and 5). During substages 5a, 5b and 5c, parallel changes in temperature and oxygen isotopes are recorded, probably reflecting D–O Interstadials 24 to 21. The relatively cold temperatures during substage 5c would be due to the occurrence of a cooling event in the Northern Hemisphere (D–O Stadial 24). This temperature decrease was between 3 and 5 °C, whereas the subsequent warming during D–O Interstadial 23 reached 4 °C in winter and up to 7 °C in summer. D–O Interstadial 22 is not clearly defined either in the paleo-SST or in the isotope data (Figs. 4 and 5).

Some of the faunal events are unambiguously related with this D–O variability: events Q10 and Sc8 are contemporaneous and developed during Stadial 21 (Fig. 3c,d), while events Q9 and Sc7 occurred at Stadial 20. Similar increases in *T. quinqueloba* and *G. scitula* occurred during younger D–O Stadials (Pérez-Folgado et al., 2003). Both species are also abundant during glacial stage 6 (around 140–150 ka; Q13 and Sc11; Fig. 3) and at Termination II (Q12).

5.1.1. The last interglacial and Termination II in the Alboran Sea

Oceanographic conditions equivalent to those existing in the present ocean occurred between 127 and 117 ka ago, during the Last Interglacial period. Greenland records show that climate in the northern hemisphere has remained very stable throughout the Holocene; however, the same records for the Last Interglacial point to great variability (Dansgaard et al., 1993; GRIP members, 1993; Grootes et al., 1993). Traditionally, substage 5e has been associated with a warm stable period (the Eemian), but Greenland ice core records (GRIP members, 1993; Grootes et al., 1993) have led to controversy that remains to be settled. GRIP ice core records seem to indicate considerable variability within the Eemian (GRIP members, 1993). However, in core GISP2, these rapid climate fluctuations do not appear and both cores show evidence of ice deformation in some parts of the core length (Alley et al., 1995). From that time onwards, many studies have been carried out on both continental (mainly from Europe) and oceanic records (especially in the North Atlantic), although with unequal results (Seidenkrantz et al., 1995; Field et al., 1994; Fronval and Jansen, 1996; Adkins et al., 1997; McManus et al., 1994; Chapman and Shackleton, 1998; Frogley et al., 1999). Although the extreme variability of Greenland ice core during substage 5e is difficult to identify in other records, it seems evident that the Eemian climate was not as stable as previously thought.

Lototskaya and Ganssen (1999) divided Termination II into two stages, T-IIa and T-IIb, with a T-II “pause” in between. This T-II pause lasted for 3 ka, and the total process lasted around 10 ka. This break in the penultimate deglaciation has also been described by other authors (Lauritzen, 1995; Sánchez-Goñi et al., 2000; Calvo et al., 2001).

Based on our oxygen isotope data, substage 5e would have taken place in the Alboran Sea between ~117 and 130 ka (Fig. 4). The isotopic drop at 130 ka is interrupted at 128 ka by a short event of slight isotopic enrichment (~0.4‰) (Fig. 4). After 127.4 ka, $\delta^{18}\text{O}$ decreased again to reach the lowest values, between 125.6 and 119.4 ka. From 119 ka upwards, a progressive increase is recorded, defining the transition between substages 5e/5d.

However, the response of the assemblages of planktic foraminifera to deglaciation is different from that recorded in the isotopes. Planktonic foraminifera were still dominated by the cold-water species during most of the deglaciation (Figs. 3–5). Characteristic taxa of interglacial times, such as *G. ruber*, *G. inflata* or the SPRUDTS group (Jorissen et al., 1993), became abundant at 127 ka; that is, once most of the isotope decrease had been completed (Fig. 4). Annual paleo-SST fluctuate around 10–11 °C between 130 and 127 ka, and then increase sharply to values close to 20 °C (slightly higher than the average recent and Holocene annual temperatures; database of Kallel et al., 1997a). This temperature increase of around 10 °C should be recorded by a 2.3‰ $\delta^{18}\text{O}$ isotope decrease, but the amplitude of the isotope change is only 0.6‰. This small change can be explained in terms of a contemporaneous reduction in the isotope composition of Mediterranean surface waters (Fig. 4). Spring paleotemperatures increased by around 8 °C during the deglaciation, from 9 to 17 °C. Kallel et al. (2000) studied planktic foraminiferal assemblages and estimated MAT paleotemperatures in two cores from the Thyrrenian Sea off Italy. The temperature rise is similar to that recorded in our sediments. Their results also seem to indicate that the isotopic drop during T-II took place before the temperature rise and the faunal change (Kallel et al., 2000). The delay in the SST increase at T-II is due to the occurrence of a prominent cold event between 133 and 128 ka, possibly associated to the influence of the Heinrich interval HE11 (Heinrich, 1988). Although with small fluctuations, the isotope and temperature records remained relatively stable during the Eemian, the highest temperatures and the lowest oxygen isotope values of the last 150 ka being reached at around 122 ka ago, when SST began to decrease progressively towards substage 5d.

5.2. Organic-rich layers in the Western Mediterranean, and their paleoceanographic implications

The ORL (sensu Comas et al., 1996) layers discovered during ODP Leg 161 in the Western Mediterranean were not considered as true sapropels, although their organic carbon content was generally higher than the average content of the overlying and underlying levels. In ODP Site 977, 52 ORLs were found (Murat, 1999), of which the uppermost eight (L1 to L8) are included in this study. The average organic matter content and location of each ORL is shown in Table 4. L1 occurs between MIS 1 and 2, L2 and L3 during MIS 3 (Fig. 3), and the rest (L4 to L8) during MIS 5. Organic matter percentages are not very high (maximum 1.13%) but are considerably higher than the background percentage for the whole core (0.55%; Comas et al., 1996; Murat, 1999).

Sapropels S3, S4 and S5 in the Eastern Mediterranean are recorded during substages 5a, 5c and 5e, respectively (see review in Cramp and O'Sullivan, 1999). In agreement with previous correlations reported by Capotondi and Vigliotti (1999), we relate ORL L4 in ODP 977 with sapropel S3, L5 and L6 with S4 and finally L7 and L8 with sapropel S5.

The estimated δw record reflects large decreases in sea-water $\delta^{18}O$ values throughout the deposition of most of the ORLs (Fig. 4). These changes are necessarily linked to drops in the δw of the inflowing Atlantic waters or to variations in the hydrological budget of the basin (Kallel et al., 1997b); that is, an increase in rainfall or runoff, which would produce a decrease in sea surface salinity. Lower sea surface salinities would have enhanced water stratification throughout the water column, which in combination with relatively high surface water productivities

would explain the higher contents of organic matter. *G. bulloides*, which typically thrive in cold, high-productivity waters (Hemleben et al., 1989; Pujol and Vergnaud-Grazzini, 1995), is relatively scarce within interglacial stage MIS 5 with the exception of glacial substage 5d. However, significant increases in abundance occur in all ORLs as illustrated by the correspondence of biological events B11, B12, B13 and B15, defined in this study, with ORLs L4, L5, L6 and L8, respectively (Fig. 3b). The combination of high percentages of *G. bulloides* during these episodes with low values of δw in surface waters seem to be related with events of high primary productivity at surface and stratification in the water column which results in the formation of the ORLs.

Cane et al. (2002) obtained high-resolution records in four cores from the Eastern Mediterranean sapropel S5. They demonstrated that some planktic foraminiferal events that occurred at the time of the deposition of S5 were remarkably isochronous throughout the Eastern Mediterranean. Events f 9 (a marked increase in the abundance of *G. ruber* pink) and f 8 (a reduction in the abundance of *G. inflata*) may be related to events R2a (125 ka) and the top of zone I11 (124 ka) in our study. Using the age model proposed by Rohling et al. (2002), events f 9 and f 8, which immediately predate and postdate the onset of sapropel S5, have an age of ~124.4 and ~123.6 ka, respectively. Assuming that events R2a and I11, which during deposition of ORL 7 in the Alboran Sea are nearly isochronous with events f 9 and f 8 and the base of S5, the onset of sapropel S5 in the Eastern Mediterranean occurred about 5 ka later than the onset of ORL 8 in the Alboran Sea. Sierro et al. (1998) identified and dated the youngest organic-rich layer of the Alboran Sea in core MD95-2043 (Fig. 1). These authors gave an age of 14.5 cal ka to the base of this sapropel-like layer. However, sapropel S1 is normally dated at ~9.5 ka (Aksu et al., 1999). The ages attributed by Rossignol-Strick and Paterne (1999) to the same events in the Ionian Sea, using the monsoon index, are also consistently younger than the sapropel-like layers in the Alboran Sea.

Bar-Matthews et al. (2000) analyzed the isotopic record of speleothems from the Soreq cave (Israel) and deduced five prominent low $\delta^{18}O$ events, related to periods of enhanced rainfall in the Eastern Mediterranean. The independently obtained (U–Th

Table 4
Organic-rich layers found in ODP 977 samples

ORL	Depth (m)	Age (kiloyears)	TOC (%)
L1	1.95–2.24	11.1–12.3	0.87
L2	5.73–7.70	28.3–37.2	1.02 (max)
L3	8.93–9.05	41.2–41.5	1.07 (max)
L4	18.08–18.24	79.3–81.3	0.93
L5	19.39–19.57	92.6–96.2	1.13
L6	20.28–20.63	100.3–102.3	0.88
L7	23.32–23.61	123.5–125.0	1.13
L8	23.85–24.30	126.8–129.8	0.79

dating) ages of four of these events correlated well with sapropel layers S5, S4, S3 and S1. The ages reported by Bar-Matthews et al. (2000) for S3 and S4 are 85–79 and 108–100 ka, respectively, whereas the ORLs are dated at about 79–81 and 92–102 ka, respectively (Table 4). Therefore, sapropels S1 and S5 are probably younger than their equivalent ORLs in the Western Mediterranean, L1 and L7–L8, whereas S3 and S4 seems to be slightly older than their equivalent ORLs, L4 and L5–L6. Nevertheless, the framework are not good constrained for S3 and S4, there are no good biosratigraphic patterns, and the offset could vary largely depending on the age models applied. The different hydrography and oceanography of the Western Mediterranean, which was strongly influenced by Atlantic signatures, and the Eastern basin could be an important factor to explain the age differences. Nevertheless, more studies and very accurate age models are needed, especially in the Western part, to elucidate the reasons of these time lags.

6. Conclusions

A micropaleontological study was carried out in hole ODP 977, drilled out in the Alboran Sea. Quantitative changes in abundance of eight planktic foraminiferal species have led us to recognize 42 biostratigraphic faunal events, between 60 and 150 ka. The results confirm that the cores retrieved from the Alboran Sea record the paleoclimatic and paleoceanographic changes of both, Atlantic Ocean and Mediterranean Sea. Rapid SST fluctuations during MIS 4–6 are related with Dansgaard–Oeschger and glacial–interglacial climatic variability. In particular, significant warmings occur during Interstadials 19 to 24 both during glacial and interglacial stages. A time lag of about 3 ka was found between the initiation of Termination II, 130 ka ago, and the warming inferred from the planktic foraminiferal assemblages. This could be related to the contemporaneous occurrence of a cold event, associated to the presence of the Heinrich interval HE11.

The deposition of ORLs L4 to L8, which occurred during MIS 5, seem to be related with sapropels S3 (L4), S4 (L5 and L6) and S5 (L7 and L8) in the Eastern Mediterranean. Depletions in δw during some

of the ORLs and high percentages of *G. bulloides* in most of them suggest that these ORLs would be related with a fresher surface layer associated with increased surface productivity. Detailed biostratigraphic correlations between Eastern and Western Mediterranean cores allow us to conclude that deposition of sapropels S1 and S5 started 5 ka earlier in the Western Mediterranean. However, more studies are needed to understand the different behavior of sapropels and ORLs along the Mediterranean transect.

Acknowledgements

We acknowledge the helpful reviews of G.J. de Lange and M.B. Cita. This work was funded by DGICYT projects PB-98-0288, FEDER 1FD1997-1148 (CLI) and BTE2002-04670, and by the Spanish Government FPI Grant FP96 11964731. We thank the Ocean Drilling Program for providing the ODP 977 samples.

References

- Adkins, J.F., Boyle, E.A., Keigwin, L.D., Cortijo, E., 1997. Variability of the North Atlantic thermohaline circulation during the last interglacial period. *Nature* 390, 154–156.
- Aksu, A.E., Abrajano, T., Mudie, P.J., Yasar, D., 1999. Organic geochemical and palynological evidence for terrigenous origin of the organic matter in Aegean Sea sapropel S1. *Marine Geology* 153, 303–318.
- Alley, R.B., Gow, A.J., Johnsen, S.J., Kipfstuhl, J., Meese, D.A., Thorsteinsson, T., 1995. Comparison of deep ice cores. *Nature* 373, 393–394.
- Bárcena, M.A., Abrantes, F., 1998. Evidence of a high-productivity area off the coast of Malaga from studies of diatoms in surface sediments. *Marine Micropaleontology* 35, 91–103.
- Bar-Matthews, M., Ayalon, A., Kaufman, A., 2000. Timing and hydrological conditions of sapropel events in the Eastern Mediterranean, as evident from the speleothems, Soreq cave, Israel. *Chemical Geology* 169, 145–156.
- Bethoux, J.P., 1979. Budgets of the Mediterranean Sea. Their dependence on the local climate and on the characteristics of the Atlantic waters. *Oceanologica Acta* 2 (2), 157–163.
- Bethoux, J.P., 1993. Mediterranean sapropel formation, dynamic and climatic viewpoints. *Oceanologica Acta* 16 (2), 127–133.
- Blunier, T., Brook, E.J., 2001. Timing of millennial-scale climate change in Antarctica and Greenland during the Last Glacial Period. *Science* 291, 109–112.
- Bond, G., Broecker, W., Johnsen, S., McManus, J., Labeyrie, L., Jouzel, J., Bonani, G., 1993. Correlations between climate

- records from North Atlantic sediments and Greenland ice. *Nature* 365, 143–147.
- Bradley, W.H., 1938. Mediterranean sediments and Pleistocene sea levels. *Science* 88, 376–379.
- Cacho, I., Grimalt, J.O., Pelejero, C., Canals, M., Sierro, F.J., Flores, J.A., Shackleton, N., 1999. Dansgaard–Oeschger and Heinrich event imprints in Alboran Sea paleotemperatures. *Paleoceanography* 14 (6), 698–705.
- Cacho, I., Grimalt, J.O., Sierro, F.J., Shackleton, N.J., Canals, M., 2000. Evidence for enhanced Mediterranean thermohaline circulation during rapid climate coolings. *Earth and Planetary Science Letters* 183, 417–429.
- Calvo, E., Villanueva, J., Grimalt, J.-O., Boelaert, A., Labeyrie, L., 2001. New insights into glacial latitudinal temperature gradients in the North Atlantic. Results from Uk' 37 sea surface temperatures and terrigenous inputs. *Earth and Planetary Science Letters* 188, 509–519.
- Cane, T.R., Rohling, E.J., Kemp, A.E.S., Cooke, S., Pearce, R.B., 2002. High-resolution stratigraphic framework for Mediterranean sapropel S5: defining temporal relationships between records of Eemian climate variability. *Palaeogeography, Palaeoclimatology, Palaeoecology* 183, 87–101.
- Capotondi, L., Vigliotti, L., 1999. Magnetic and microfaunal characterization of Late Quaternary sediments from the Western Mediterranean: inferences about sapropel formation and paleoceanographic implications. In: Zahn, R., Comas, M.C., Klaus, A., (Eds.), *Proceedings of the Ocean Drilling Program, Scientific Results*, vol. 161. Ocean Drilling program, College Station, TX, pp. 505–518.
- Cayre, O., Lancelot, Y., Vincent, E., Hall, M.A., 1999. Paleoceanographic reconstructions from planktonic foraminifera off the Iberian Margin: temperature, salinity, and Heinrich events. *Paleoceanography* 14 (3), 384–396.
- Chapman, M.R., Shackleton, N.J., 1998. Millennial-scale fluctuations in North Atlantic heat flux during the last 150,000 years. *Earth and Planetary Science Letters* 159, 57–70.
- Chapman, M.R., Shackleton, N.J., 1999. Global ice-volume fluctuations, North Atlantic ice-rafting events, and deep-ocean circulation changes between 130 and 70 ka. *Geology* 27, 795–798.
- Comas, M., Zahn, R., Klaus, A., 1996. *Proc. ODP Init. Results* 161, 1023 pp.
- Cramp, A., O'Sullivan, G., 1999. Neogene sapropels in the Mediterranean: a review. *Marine Geology* 153, 11–28.
- Dansgaard, W., Johnsen, S.J., Clausen, H.B., Dahl-Jensen, D., Gundestrup, N.S., Hammer, C.V., Hvidberg, C.S., Steffensen, J.P., Sveinbjornsdottir, A.E., Jouzel, J., Bard, G., 1993. Evidence for general instability of past climate from a 250 kyr ice-core record. *Nature* 364, 218–220.
- Duplessy, J.C., Labeyrie, L., Juillet-Leclerc, A., Maitre, F., Duprat, J., Sarnthein, M., 1991. Surface salinity reconstruction of the North Atlantic Ocean during the last glacial maximum. *Oceanologica Acta* 14 (4), 311–324.
- Emeis, K.C., Robertson, A.H.F., Richter, C., 1996. *Init. Results of the Ocean Drilling Program*, vol. 160. Ocean Drilling Program, College Station, TX, 972 pp.
- Eynaud, F., Turon, J.-L., Sánchez-Goñi, M.F., Gendreau, S., 2000. Dinoflagellate cyst evidence of 'Heinrich-like events' off Portugal during the Marine Isotopic Stage 5. *Marine Micropaleontology* 40, 9–21.
- Field, M.H., Huntley, B., Müller, H., 1994. Eemian climate fluctuations observed in a European pollen record. *Nature* 371, 779–783.
- Frogley, M.R., Tzedakis, P., Heaton, T.H.E., 1999. Climate variability in Northwest Greece during the last interglacial. *Science* 285, 1886–1889.
- Fronval, T., Jansen, E., 1996. Rapid changes in ocean circulation and heat flux in the Nordic Seas during the last interglacial period. *Nature* 383, 806–810.
- Ganssen, G., Troelstra, S.R., 1987. Paleoenvironmental changes from stable isotopes in planktonic foraminifera from eastern Mediterranean sapropels. *Marine Geology* 75, 221–230.
- García-Gorriñ, E., Carr, M.-E., 2001. Physical control of phytoplankton distributions in the Alboran Sea: a numerical and satellite approach. *Journal of Geophysical Research* 106 (C8), 16795–16805.
- Greenland Ice-Core Project (GRIP) members, 1993. Climate instability during the last interglacial period recorded in the GRIP ice core. *Nature* 364, 203–207.
- Groote, P.M., Stuiver, M., White, J.W.C., Johnsen, S., Jouzel, J., 1993. Comparison of oxygen isotope records from the GISP2 and GRIP Greenland ice cores. *Nature* 366, 552–554.
- Heburn, G.W., LaViolette, P.E., 1990. Variations in the structure of the Anticyclonic Gyres found in the Alboran Sea. *Journal of Geophysical Research* 95 (C2), 1599–1613.
- Heinrich, H., 1988. Origin and consequences of cyclic ice rafting in the Northeast Atlantic Ocean during the past 130,000 years. *Quaternary Research* 29, 142–152.
- Hemleben, C., Spindler, M., Anderson, O.R., 1989. *Modern Planktonic Foraminifera*. Springer, New York.
- Hsü, K., Montadert, L., et al., 1978. *Initial Reports of the Deep Sea Drilling Project*, vol. 42. U.S. Government Printing Office, Washington.
- Hüls, M., Zahn, R., 2000. Millennial-scale sea surface temperature variability in the western tropical North Atlantic from planktonic foraminiferal census counts. *Paleoceanography* 15, 659–678.
- Hutson, W.H., 1980. The Agulhas current during the Late Pleistocene: analysis of modern faunal analogs. *Science* 207, 64–66.
- Jorissen, F.J., Asioli, A., Borsetti, A.M., Capotondi, L., de Visser, J.P., Hilgen, F.J., Rohling, E.J., van der Borg, K., Vergnaud-Grazzini, C., Zachariasse, W.J., 1993. Late Quaternary central Mediterranean biochronology. *Marine Micropaleontology* 21, 169–189.
- Kallel, N., Paterne, M., Duplessy, J.C., Vergnaud-Grazzini, C., Pujol, C., Labeyrie, L., Arnold, M., Fontugne, M., Pierre, C., 1997a. Enhanced rainfall in the Mediterranean region during the last sapropel event. *Oceanologica Acta* 20, 697–712.
- Kallel, N., Paterne, M., Labeyrie, L., Duplessy, J.-C., Arnold, M., 1997b. Temperature and salinity records of the Tyrrhenian Sea during the last 18,000 years. *Palaeogeography, Palaeoclimatology, Palaeoecology* 135, 97–108.
- Kallel, N., Duplessy, J.-C., Labeyrie, L., Fontugne, M., Paterne, M., Montacer, M., 2000. Mediterranean pluvial periods and sapropel formation over the last 200,000 years. *Palaeogeography, Palaeoclimatology, Palaeoecology* 157, 45–58.

- Kanfoush, S.L., Hodell, D.A., Charles, C.D., Guilderson, T.P., Mortyn, P.G., Ninnemann, U.S., 2000. Millennial-scale instability of the Antarctic Ice Sheet during the last glaciation. *Science* 288, 1815–1818.
- Kidd, R.B., Cita, M.B., Ryan, W.B.F., 1978. Stratigraphy of eastern Mediterranean sapropel sequences recovered during Leg 42A and their paleoenvironmental significance. *Init. Rep. DSDP 42A*, 421–443.
- Kinder, T.H., Parrilla, G., 1987. Yes, some of the Mediterranean outflow does come from great depth. *Journal of Geophysical Research* 95 (C3), 2901–2906.
- Kullenberg, B., 1952. On the salinity of the water contained in marine sediments. *Meddelanden Oceanografiska Goteborg* 21, 1–38.
- Lauritzen, S.E., 1995. High-resolution paleotemperature proxy record for the Last Interglaciation based on Norwegian speleothems. *Quaternary Research* 43, 133–146.
- Lehman, S.J., Sachs, J.P., Crotwell, A.M., Keigwin, L.D., Boyle, E.A., 2002. Relation of subtropical Atlantic temperature, high-latitude ice-rafting, deep water formation, and European climate 130,000–60,000 years ago. *Quaternary Science Reviews* 21, 1917–1924.
- Little, M.G., Schneider, R.R., Kroon, D., Price, B., Summerhayes, C.P., Segl, M., 1997. Trade wind forcing of upwelling, seasonality, and Heinrich events as a response to sub-Milankovitch climate variability. *Paleoceanography* 12 (4), 568–576.
- Lototskaya, A., Ganssen, G.M., 1999. The structure of Termination II (penultimate deglaciation and Eemian) in the North Atlantic. *Quaternary Science Reviews* 18, 1641–1654.
- Martinson, D.G., Pisias, N.G., Hays, J.D., Imbrie, J., Moore, T.C., Shackleton, N.J., 1987. Age dating and the orbital theory of the ice ages: development of a high-resolution 0 to 300,000-year chronostratigraphy. *Quaternary Research* 27, 1–29.
- McManus, J.F., Bond, G.C., Broecker, W.S., Johnsen, S., Labeyrie, L., Higgins, S., 1994. High-resolution climate records from the North Atlantic during the last interglacial. *Nature* 371, 326–329.
- McManus, J.F., Oppo, D.W., Cullen, J.L., 1999. A 0.5-million-year record of millennial-scale climate variability in the North Atlantic. *Science* 283, 971–975.
- Meyers, P.A., Negri, A. (Eds.), 2003. Special issue: paleoclimatic and paleoceanographic records in Mediterranean sapropels and Mesozoic black shales, *Palaeogeography, Palaeoclimatology, Palaeoecology* 190, 480 pp.
- Murat, A., 1999. Pliocene–Pleistocene occurrence of sapropels in the Western Mediterranean Sea and their relation to Eastern Mediterranean sapropels. In: Zahn, R., Comas, M.C., Klaus, A., (Eds.), *Proceedings of the Ocean Drilling Program, Scientific Results*, vol. 161. Ocean Drilling Program, College Station, TX, pp. 519–527.
- Oppo, D.W., Horowitz, M., Lehman, S.J., 1997. Marine core evidence for reduced deep water production during Termination II followed by a relatively stable substage 5e (Eemian). *Paleoceanography* 12 (1), 51–63.
- Oppo, D.W., Keigwin, L.D., McManus, J.F., Cullen, J.L., 2001. Persistent suborbital climate variability in marine isotope stage 5 and Termination II. *Paleoceanography* 16 (3), 280–292.
- Overpeck, J.T., Webb III, T., Prentice, I.C., 1985. Quantitative interpretation of Fossil Pollen Spectra: dissimilarity coefficients and the method of Modern Analog. *Quaternary Research* 23, 87–108.
- Parrilla, G., 1984. Preliminary results of the “¿Donde Va? experiment.” *Informe Técnico* 24, Inst. Esp. Oceanog. (Madrid, España), 264 pp.
- Parrilla, G., Kinder, T.H., 1987. *Oceanografía física del Mar de Alborán*. *Boletín del Instituto Español de Oceanografía* 4 (1), 133–165.
- Pérez-Folgado, M., Sierro, F.-J., Flores, J.A., Cacho, I., Grimalt, J.-O., Zahn, R., Shackleton, N.J., 2003. Western Mediterranean planktic foraminifera events and millennial climatic variability during the last 70 kiloyears. *Marine Micropaleontology* 48, 49–70.
- Prell, W.L., 1985. The stability of low-latitude sea-surface temperatures: An evaluation of the CLIMAP reconstruction with emphasis on the positive SST anomalies., U.S. Department of Energy. Technical Report (TRO25), Brown University, Dept. of Applied Sciences, 60 pp.
- Pujol, C., Vergnaud-Grazzini, C., 1989. Paleocyanography of the Last Deglaciation in the Alboran Sea (Western Mediterranean). Stable isotopes and planktonic foraminiferal records. *Marine Micropaleontology* 15, 153–179.
- Pujol, C., Vergnaud-Grazzini, C., 1995. Distribution patterns of live planktic foraminifers as related to regional hydrography and productive systems of the Mediterranean Sea. *Marine Micropaleontology* 25, 187–217.
- Rohling, E.J., 1994. Review and new aspects concerning the formation of eastern Mediterranean sapropels. *Marine Geology* 122, 1–28.
- Rohling, E.J. (Ed.), 1999. Special issue: Fifth decades of Mediterranean Paleoclimate and Sapropel studies, *Marine Geology* 153(1–4), 350 pp.
- Rohling, E.J., 2000. Paleosalinity: confidence limits and future applications. *Marine Geology* 163, 1–11.
- Rohling, E.J., Cane, T.R., Cooke, S., Sprovieri, M., Boulabassi, I., Emeis, K.C., Schiebel, R., Kroon, D., Jorissen, F.J., Lorre, A., Kemp, A.E.S., 2002. African monsoon variability during the previous interglacial maximum. *Earth and Planetary Science Letters* 202, 61–75.
- Rohling, E.J., Mayewski, P.A., Challenor, P., 2003. On the timing and mechanism of millennial-scale climate variability during the last glacial cycle. *Climate Dynamics* 20, 257–267.
- Rosignol-Strick, M., 1985. Mediterranean Quaternary sapropels, an immediate response of the African monsoon to variation of insolation. *Palaeogeography, Palaeoclimatology, Palaeoecology* 49, 237–263.
- Rosignol-Strick, M., Paterne, M., 1999. A synthetic pollen record of the eastern Mediterranean sapropels of the last 1 Ma: implications for the time-scale and formation of sapropels. *Marine Geology* 153, 221–237.
- Ryan, W.B.F., Hsü, K.J., et al., 1973. *Initial Reports of the Deep Sea Drilling Project*, vol. 13. U.S. Government Printing Office, Washington.
- Sánchez-Goñi, M.F., Eynaud, F., Turon, J.L., Shackleton, N.J., 1999. High resolution palynological record off the Iberian margin: direct land-sea correlation for the Last Interglacial complex. *Earth and Planetary Science Letters* 171, 123–137.

- Sánchez-Goñi, M.F., Turon, J.-L., Eynaud, F., Shackleton, N.J., Cayre, O., 2000. Direct land/sea correlation of the Eemian, and its comparison with the Holocene: a high-resolution palynological record off the Iberian margin. *Netherlands Journal of Geosciences* 79, 345–354.
- Sánchez-Goñi, M.F., Cacho, I., Turon, J.-L., Guiot, J., Sierro, F.J., Peyrouquet, J.P., Grimalt, J.O., Shackleton, N.J., 2002. Synchronicity between marine and terrestrial responses to millennial scale climate variability during the last glacial period in the Mediterranean region. *Climate Dynamics* 19, 95–105.
- Schwander, J., Sowers, T., Barnola, J.M., Blunier, T., Fuchs, A., Malaizé, B., 1997. Age scale of the air in the summit ice: Implication for glacial–interglacial temperature change. *Journal of Geophysical Research* 102 (D16), 19483–19493.
- Seidenkrantz, M.-S., Kristensen, P., Knudsen, K.L., 1995. Marine evidence for climatic instability during the last interglacial records from the northwest Europe. *Journal of Quaternary Science* 10, 77–82.
- Shackleton, N.J., 1974. Attainment of isotopic equilibrium between ocean water and the benthonic foraminifera genus *Uvigerina*: isotopic changes in the ocean during the last glacial. *Colloque CNRS*, vol. 219. Centre National de la Recherche Scientifique, Paris, pp. 203–210.
- Sierro, F.J., Bárcena, M.A., Flores, J.A., Cacho, I., Pelejero, C., Grimalt, J.O., Shackleton, N.J., 1998. Origin of the youngest western Mediterranean organic-rich layer: productivity or stagnation? 6th International Conference on Paleoceanography. Volume of Abstracts, p. 211.
- Sierro, F.J., Flores, J.A., Bárcena, M.A., Vázquez, A., Utrilla, R., Zamarreño, I., 2003. Astronomical oscillations in the planktonic communities and cyclical changes in water-column stability during Messinian sapropels. *Palaeogeography, Palaeoclimatology, Palaeoecology* 190, 289–316.
- Sowers, T., Bender, M., Labeyrie, L., Martinson, D., Jouzel, J., Raynaud, D., Pichon, J.-J., Korotkevich, Y.S., 1993. A 135,000 year Vostok–Specmap common temporal framework. *Paleoceanography* 8 (6), 737–766.
- Tintoré, J., LaViolette, P., Blade, I., Cruzado, A., 1988. A study of an intense density front in the Eastern Alboran Sea: the Almería–Orán front. *Journal Physical Oceanography* 18, 1384–1397.
- Vergnaud-Grazzini, C., Devaux, M., Znidi, J., 1986. Stable isotopes “anomalies” in the Mediterranean Pleistocene records. *Marine Micropaleontology* 10, 35–69.
- Voelker, A.H.L., et al., 2002. Global distribution of centennial-scale records for Marine Isotope Stage (MIS) 3: a database. *Quaternary Science Reviews* 21, 1185–1212.